

Dynamic Rock Type Characterization Using Artificial Neural Networks in Hamra Quartzites Reservoir: A Multidisciplinary Approach

Abdallah Sokhal

Department of Geophysics, Faculty of Earth Sciences and Country Planning, University of Science and Technology Houari Boumediene, Algiers, Algeria
abdallahsokhal@gmail.com

Sid-Ali Ouadfeul

Department of Geophysics, Faculty of Earth Sciences and Country Planning, University of Science and Technology Houari Boumediene, Algiers, Algeria
souadfeul@ymail.com

Zahia Benaissa

Department of Geophysics, Faculty of Earth Sciences and Country Planning, University of Science and Technology Houari Boumediene, Algiers, Algeria
zabendz@yahoo.fr

Amar Boudella

Department of Geophysics, Faculty of Earth Sciences and Country Planning, University of Science and Technology Houari Boumediene, Algiers, Algeria
amboudella@yahoo.fr

Abstract—A new multidisciplinary workflow is suggested to re-characterize the Hamra Quartzite (QH) formation using artificial neural networks. This approach involves core description, routine core analysis, special core analysis and raw logs of fourteen wells. An efficient electrofacies clustering neural network technology based on a self-organizing map is performed. The inputs in the model computation are: neutron porosity, gamma ray and bulk density logs. According to the self-organizing map results, the reservoir is composed of five electrofacies (EF1 to EF5): EF1, EF2 and EF3 with good reservoir quality, EF4 with moderate quality, and EF5 with bad quality. Hydraulic flow units are determined from well logs and core data using the flow zone indicator (FZI) approach and the multilayer perception (MLP) method. Obtained results indicate eight optimal hydraulic flow units. Hydraulic flow units for uncored well are determined using the MLP, the used inputs to train the neural system are: neutron porosity, gamma ray, bulk density and predefined electrofacies. A dynamic rock typing is achieved using the FZI approach and combining special core data analysis to better characterize the hydraulic reservoir behavior. A best-fit relationship between water saturation and J-function is established and a good saturation match is obtained between capillary pressure and interpreted log results.

Keywords—flow zone indicator (FZI); hydraulic flow unit (HFU); multi-layer perception (MLP); self-organizing map (SOM); electrofacies (EF); J-function; lithofacies

I. INTRODUCTION

A crucial step in building a geological model is the assignment of petrophysical properties (porosity, permeability, fluid saturations) in the model cells between and beyond the existing well control [1]. The previous geological models of

Hamra Quartzites (QH) fail to accurately classify and make estimations of the reservoir's petrophysical properties [2]. As part of the updating of the geological model of QH in the Hassi Messaoud (HMD) southern periphery oil field, it would be interesting to refine the previous definitions of rock types. Reservoir rock typing should be a cooperative procedure between various disciplines such as geology, petrophysics and reservoir engineering [3]. These specialties have diverse definitions of rock types because of their different work scales. The authors provide many terminologies of rock types such as lithofacies, electrofacies (EF) and hydraulic flow unit (HFU). Geologists characterize lithofacies based on similar diagenetic process and depositional environment [4], petrophysicists determine EFs based on the same responses of log measurements in a well and reservoir engineers describe HFUs based on the identical pore size distribution and pore throat size [5]. These disciplines are not studying the rock types in the same manner and also there is a complex correlation between terminologies due to dimensionality problems [3]. The challenge is to choose a reference between these rock types, keeping in mind that raw log data have a restricted resolution and depend on environmental conditions [6], routine core data and core description have a lacking coverage and are sensitive to interpretation [3]. Artificial neural network (ANN) approaches are often employed in reservoir characterization dealing with EF and HFU modeling [7-9]. They are powerful tools in reservoir nonlinearity examination [10]. This ability grades ANN among the most used clustering and classification methods [11]. In literature, the self-organizing map (SOM) is performed to delineate EFs present in the reservoir [12]. Multi-layer perception (MLP) neural networks have been recognized as universal function approximators [9, 13].

Corresponding author: Abdallah Sokhal

www.etasr.com

Sokhal et al.: Dynamic Rock Typing Characterization Using Artificial Neural Networks in Hamra ...

In this study, we present a multidisciplinary workflow for dynamic rock typing in reservoir characterization based on core description, well logs, routine core analysis (RCA) and special core analysis (SCAL). First, the lithofacies are derived from the grain size, the bioturbation and the silicification. Then, an unsupervised ANN SOM clustering algorithm is performed to delineate EFs present in the QH reservoir. Next, a capillary pressure (PC) based rock typing is performed using SCAL, PC and pore throat radius (PTR) distributions available in one well for the QH reservoir. After that, HFUs are determined from core data using flow zone indicator (FZI) approach, a supervised ANN MLP algorithm is carried out to determine the permeability in un-cored wells. Finally, a saturation height modeling (SHM) is performed and an equation for estimating water saturation as a function of height in a reservoir based on capillarity concepts is provided.

II. GEOLOGICAL CONTEXT AND LITHOFACIES DETERMINATION

The QH reservoir is located on lower Ordovician formations, it is a newly proven oil play in the HMD southern periphery oil field. The Cambro-Ordovician stratigraphic sequence of the HMD oil field consists of a siliciclastic series unconformably overlying an eruptive metamorphic basement (Figure 1) [14]. The QH reservoir is divided in six zones (QH_1 to QH_6) which are partially or totally eroded by the Hercynian tectonic phases. This subdivision is mainly based on logging responses and, in particular, on the GR logs [15].

The sedimentation of QH is dominated by sandstones which are intensively bioturbated (skolithos, pipes-rock) and underwent during their burial history an important quartz cementation which modified their mechanical properties and porosity [16]. The cores were used to define lithofacies based on the grain size, the bioturbation and the silicification. These lithofacies are deposited in foreshore, upper shoreface and proximal/middle to distal/middle shoreface environments. The lithofacies 1 and 2 are deposited in foreshore to upper shoreface environment. They appear to be shaly and consist of very fine sandstones with low porosity and which end with clay. They belong to the base of the QH. The lithofacies 3 and 4 are deposited in proximal/middle shoreface environment. They consist of fine-to-medium sandstones with wide burrow and tigilites with low silicification. These two lithofacies, which usually present the best rock qualities, correspond to the middle part of the QH. The lithofacies 5 is deposited in distal/middle shoreface. It is described as fine sandstones, more homogeneous, highly silicified and surmounted by sandstones which are rich in microstylolites. It belongs to the upper part of the QH.

III. METHODOLOGY AND DATA

The objective of this work is to propose a multidisciplinary workflow for dynamic rock type characterization. This approach includes several steps.

A. Electrofacies Determination

The expression EF was defined as a set of raw well log answers which describes a portion of the reservoir and allows differentiation from the properties of other rock volumes [17]. The EF classification has been used to guide the distribution of petrophysical properties in the geological model, in a manner that reflects significant distinctions in reservoir characteristics and spatial framework which are consistent with the geologic controls on these characteristics. In the studied QH reservoir, we have applied the unsupervised method SOM for EF classification. In an unsupervised learning, the network does not receive any information from the environment indicating what should be its output. Thus, the network itself must discover the correlations between the learning patterns. Cells and connections must reach a certain degree of self-organization [12]. The Kohonen SOM is usually composed of a two-dimensional neuronal grid (Figure 2). It offers the possibility to perform reduction in dimensions by projecting multidimensional data on a two or three dimension map. Each neuron i of the output layer has a neighborhood in this space [18] and has recurrent lateral connections in its layer (the neuron inhibits the distant neurons and lets act the neighboring ones). This type of neural network is mainly used in classification through an unsupervised learning Kohonen algorithm [7, 18, 19, 23]. If we name W_i the vector of the connections, or vector of weight, connecting the input vector Z of the input layer to the neuron i of the output layer, the whole dataset W_i constitutes the SOM parameters which are determined during the learning phase. The learning takes place in a predefined number of cycles which correspond to the presentation of the set of observations to the network.

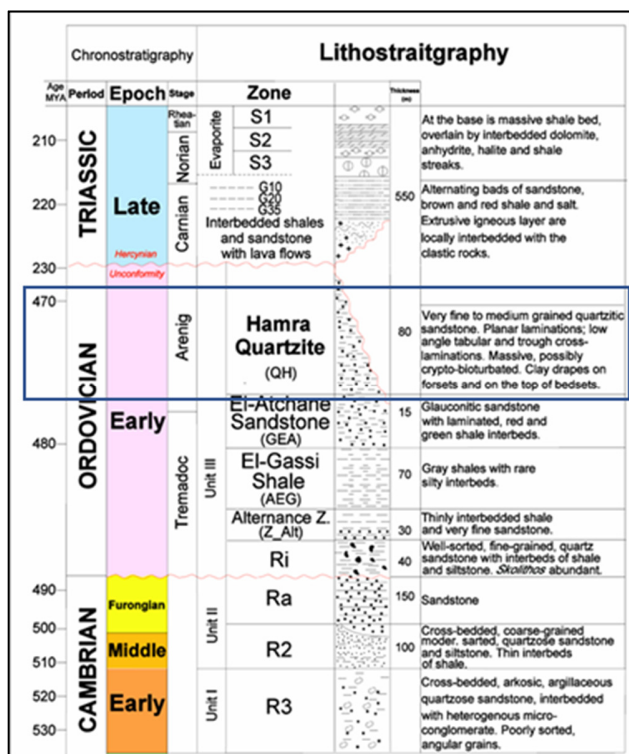


Fig. 1. Paleozoic section of the HMD southern periphery oil field, Algeria.

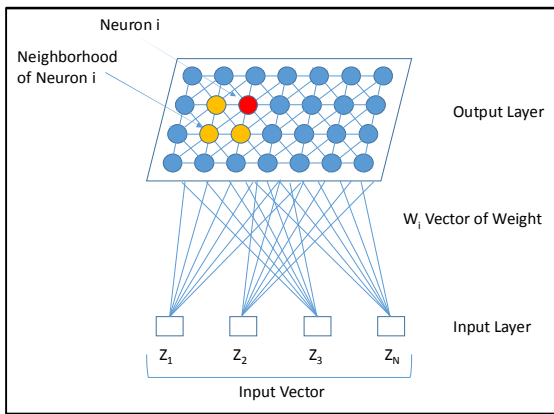


Fig. 2. Concept of the SOM method.

In this study, we use the Ipsom module of Techlog. It provides an automatic unsupervised classification solution which is based on the neural network technology (Kohonen algorithm). The input data concern the raw well logs data such as neutron porosity log (NPHI), bulk density log (RHOB) and gamma ray log (GR) and the outputs are the map and the optimal number of EFs. The first stage corresponding to the learning phase will identify the existing EFs in a select group of six model wells and the second stage will be to apply these EFs determined from the model wells to the eight remaining wells with the appropriate sequence of logs.

B. Hydraulic Flow Unit Determination

The expression HFU was defined as a mappable part of the reservoir with some particular geologic and petrophysical features that affect fluid flow [20, 21]. So, if we subdivide the reservoir into HFUs, permeability can be predicted with sufficient accuracy. The main purpose of this work is to determine the flow units in the QH reservoir. Authors in [20] declared that core data measurements give information about depositional and diagenetic features which control the variations in pore geometry which leads to hydraulic flow units with the same flow properties. Their proposed method is focused on Cozeny-Karmen equation, so, by using a various combination of petrophysical, geologic and statistical analyses, flow units are associated to well log responses to build regression models for permeability estimations in the un-cored wells. Each HFU is characterized by a single flow zone indicator (FZI), which also depends on the reservoir quality index (RQI) and void ratio ϕ_z [22, 24, 25]. These three parameters are defined according to the following equations:

$$RQI = 0.0314 \times \sqrt{\frac{K}{\phi_e}} \quad (1)$$

$$\phi_z = \frac{\phi_e}{1 - \phi_e} \quad (2)$$

$$FZI = \frac{1}{\sqrt{F_s \tau S_{gv}}} = \frac{RQI}{\phi_z} \quad (3)$$

where ϕ_e is the effective porosity in fraction, K is the permeability in mD, RQI is the reservoir quality index in μm , ϕ_z is the normalized porosity index, FZI is the flow zone indicator in μm , F_s is the shape factor, τ is the tortuosity, S_{gv} is

the surface area per unit grain in μm . The permeability in mD can be calculated as:

$$K = 1014 \times FZI_{\text{Mean}}^2 \times \frac{\phi_e^2}{(1 - \phi_e)^2} \quad (4)$$

The flow unit determination methods that have the most popularity are stratigraphic modified Lorenz plot (SMLP), Winland R35 and flow zone indicator (FZI) [24, 25]. In this study, we only focus on the FZI, thus, after calculating parameters of RQI and FZI from core data, HFUs can be differentiated on the basis of FZI values. Several clustering methods can be applied for FZI zoning. The most popular are Log-Log plot of RQI vs ϕ_z , histogram analysis of FZI distribution and the probability plot of FZI distribution. In this paper, the number of HFUs is obtained by Lorenz plots. In un-cored wells, the HFUs can be estimated using a MLP approach, a computation mathematical model is built between input and output data. The used inputs to train the MLP system are: NPHI, GR, RHOB logs and predefined EFs. The calculated FZI values are used as an output.

C. Capillary Pressure and Saturation Height Modeling

A capillary pressure (PC) based rock typing is performed using SCAL, PC and pore throat radius (PTR) distributions available in one well for the QH reservoir. A saturation height modeling is an equation for estimating water saturation as a function of height in a reservoir based on capillarity concepts. It is important for volumetric calculations and it is performed by geoscientist to predict the saturation in the reservoir for a given height above the free water level.

IV. RESULTS AND DISCUSSION

A. Determination of the EFs on Learning Wells

Recorded log data of 6 wells located in the HMD southern periphery were used as models in the learning phase. They are chosen on the basis of their stratigraphic and geographic coverage and the quality and reliability of their measurements. According to core description and sedimentary environments, four tests clusters (3, 4, 5 and 6) were tried, assessed and compared. The results with five clusters highlight a good differentiation of EFs on the GR-NPHI and GR-RHOB cross plots (Figure 3(a)-3(b)), while there is insignificant overlap in the RHOB-NPHI cross plot (Figure 3(c)). This mode provides the best combination on both statistical and geologic grounds with comparison to core data and the review of EF distributions in the geological model. The mean log values of the five EFs in the model wells are summarized on Table I, the QH reservoir appears composed of five EFs: EF1, EF2 and EF3 are similar to clean sandstones with different rock qualities (very porous, porous and compact sandstone), EF4 is shaly sandstone and EF5 is shale.

B. Propagation of the EFs to Other Wells

The determined EFs are propagated, in our case, to 10 wells having the same set of logs (GR, NPHI and RHOB) as the learning wells. The results, for one well, are shown in Figure 4. A systematic quality control of the results was performed by examining each well predicted EFs distribution (Figure 4(g)) and their associated probabilities (Figure 4(h)). The probability of each EF appears very high (>65%), however, some intervals

show a probabilistic distribution less than 40%. The EF3, with the best reservoir quality, is prevalent in the middle part of the QH, from 3400m to 3430m depth (Figure 4(g)). This is in complete agreement with the previous geological and sedimentary study.

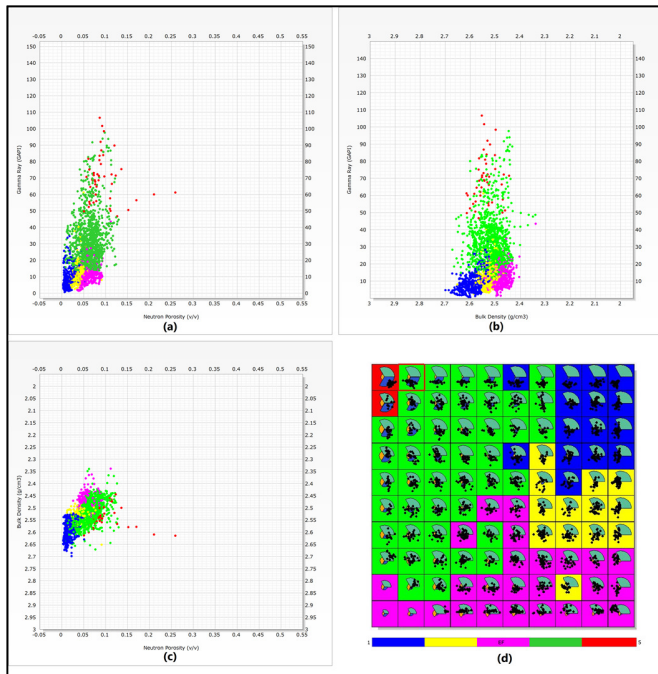


Fig. 3. EF clustering results corresponding to five clusters, during the learning phase (QH, HMD oil field southern periphery): (a) cross plot GR-NPHI, (b) cross plot GR-RHOB, (c) cross plot RHOB-NPHI, and (d) Map projection.

TABLE I. MEAN LOG VALUES OF THE 5 EFS DETERMINED BY SOM DURING THE LEARNING PHASE

EF	Average GR GAPI	Average RHOB g/cm ³	Average NPHI v/v
EF1	8.3	2.58	0.015
EF2	10.1	2.53	0.037
EF3	11.5	2.48	0.060
EF4	30	2.51	0.065
EF5	70	2.58	0.090

C. Capillary Pressure Based Dynamic Rock Typing

In this step, the SCAL and PC data are available in one well of the QH reservoir. A PC data inventory is carried out, these data are loaded for data quality control. They are edited and corrected where issues with naming conventions units and inconsistent measurements are identified. Water saturation is plotted against PC in cross plots to check the shape and trend of the PC curves. Pore throat radius (PTR) distributions are integrated with capillary pressure data (curve trend, shape and irreducible water saturation range) to identify 3 HFUs (Figure 5(a)-(b)).

D. FZI Estimation in Cored Well

Figure 6 shows a modified Lorenz plot generated for the HMD oil field southern periphery, which seems to suggest the

presence of 5 or 9 possible HFUs from the observed inflexion points. Information obtained from lithofacies, EF analysis and PC based rock typing is integrated with FZI approach to classify QH reservoir into eight HFUs. However, a clear trend particular to each HFU is observed. No PC data exists for HFU1, HFU5, HFU6, HFU7 and HFU8 for QH reservoir. The HFU classification for this case is mainly driven by FZI correlation.

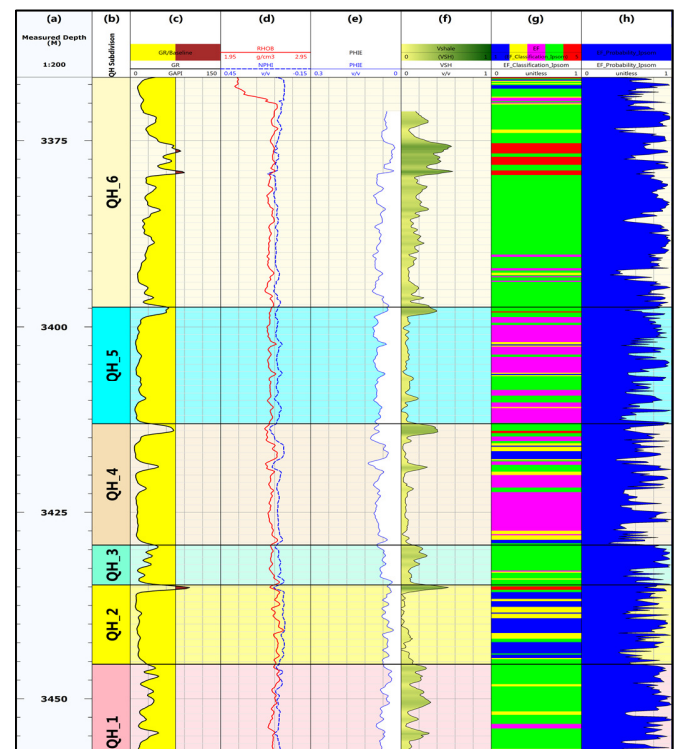


Fig. 4. Results after propagation of the 5 EFs determined by SOM to a well (QH, HMD oil field southern periphery): (a) measured depth, (b) QH subdivision, (c) GR log, (d) RHOB and NPHI logs, (e) PHIE log, (f) VSH log, (g) EF distribution, and (h) predicted probability associated to each EF.

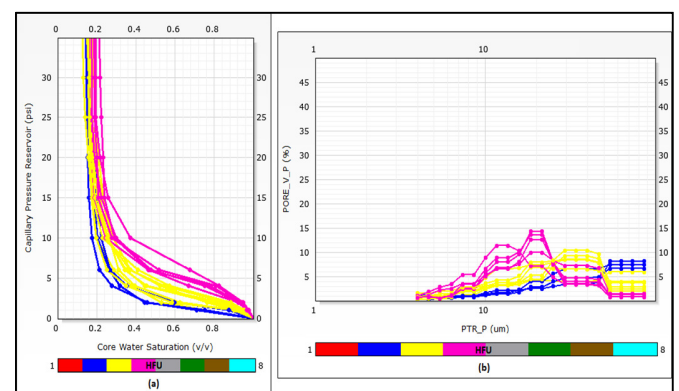


Fig. 5. PC based analysis showing 3 HFUs (QH, HMD oil field southern periphery): (a) water saturation-PC curves cross plot, (b) pore throat radius (PTR) distribution.

Figure 7 shows a composite plot of core porosity and permeability including PC data from all cored wells against

their respective FZI. The best quality rocks correspond to the red shaded points having the highest FZI values while the brown and cyan points represent the poorer quality rocks. As it is clearly indicated in Figure 8, this approach provides a very sufficient classification for the considered data. Polyline based on FZI is then fitted through the different HFUs to define porperm relationships specific to each HFU. These relations are subsequently used in the geological model to propagate permeability across the field.

consisting of 8 HFUs are investigated in terms of their stratigraphic and geographic distributions and the corresponding routine core analysis (RCA) petrophysical measurements. The rock typing distribution is showing a very clear and lateral variation of the reservoir quality. There is a strong stratigraphic control on the abundance of the HFUs with the best quality identified as HFU1, HFU2 and HFU3. These are mainly located in the zones QH_2 and QH_4 for QH reservoir (Figure 8). Above these intervals, the bad rock types are dominant.

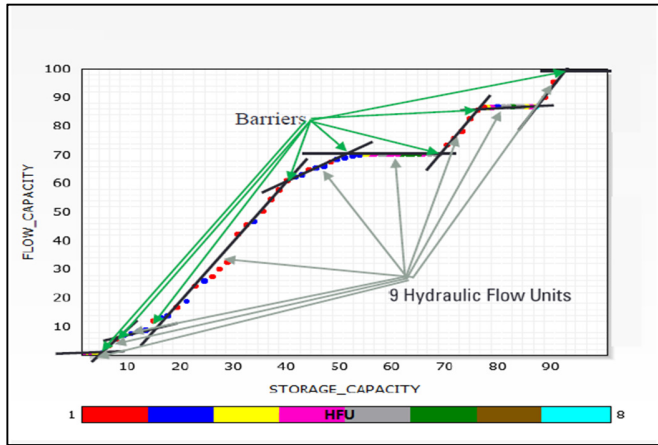


Fig. 6. Flow capacity-storage capacity Lorenz plot (QH, HMD oil field southern periphery)

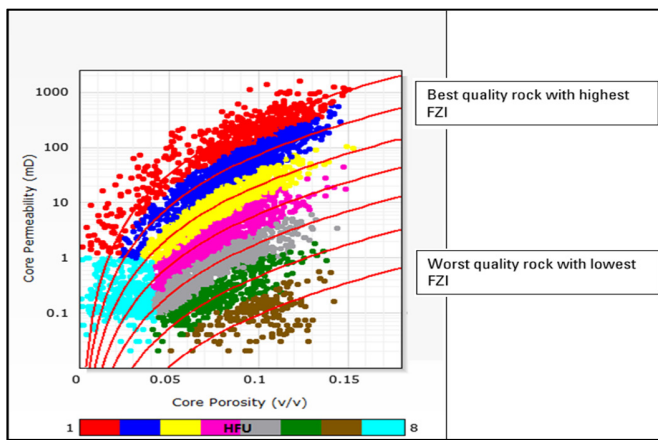


Fig. 7. Composite plot of core porosity and core permeability from all cored wells against their respective FZI (QH, HMD oil field southern periphery)

For each HFU (from HFU1 to HFU7) one equation of core permeability vs core porosity vs FZI is determined except for the HFU8, since the FZI is not applied on it. So, the HFU8 is defined like a very bad HFU with permeability less than 1mD and porosity less than 4%. The equations based on FZI correlation which provide the best poro-perm relationship for QH reservoir are summarized in Table II, in which, it can be seen that the correlation coefficient R^2 of each correlation clearly indicates the accuracy of HFU approach in permeability correlating with porosity. As part of the validation and quality control aspects of the rock typing, the cluster analysis results,

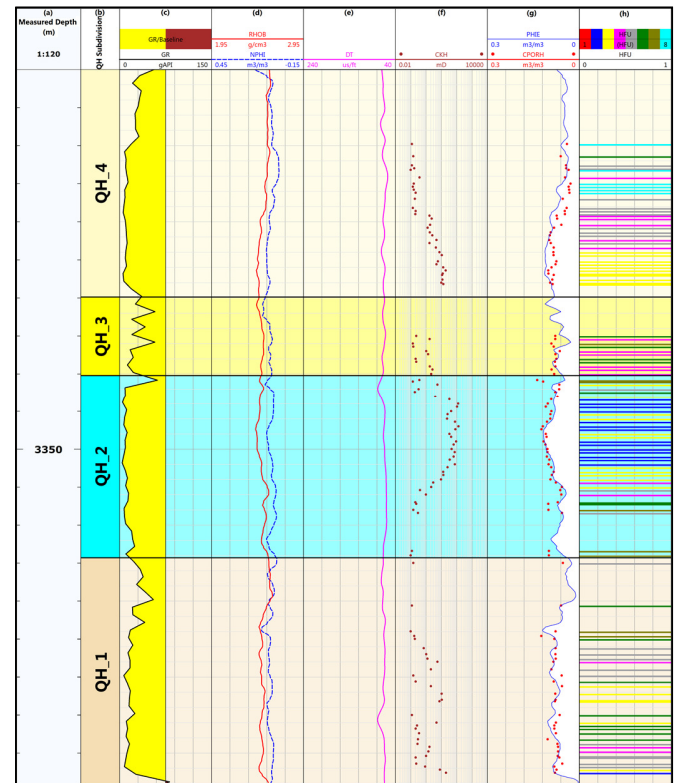


Fig. 8. Results after determination of the 8 HFUs determined by FZI method to a well (QH, HMD oil field southern periphery): (a) measured depth, (b) QH subdivision, (c) GR log, (d) RHOB and NPHI logs, (e) DT log, (f) core permeability, (g) core porosity and PHIE log, and (h) distribution of HFUs in cored interval

TABLE II. PORO-PERM RELATIONSHIP FOR QH RESERVOIR

HFU	Color	R^2	Equation
HFU1	Red	0.84	$CKH = 15^2 \times CPORH^3 / 0.0314^2 / (1 - CPORH)^2$
HFU2	Blue	0.92	$CKH = 7.6^2 \times CPORH^3 / 0.0314^2 / (1 - CPORH)^2$
HFU3	Yellow	0.96	$CKH = 4^2 \times CPORH^3 / 0.0314^2 / (1 - CPORH)^2$
HFU4	Purple	0.95	$CKH = 2.2^2 \times CPORH^3 / 0.0314^2 / (1 - CPORH)^2$
HFU5	Grey	0.85	$CKH = 1.2^2 \times CPORH^3 / 0.0314^2 / (1 - CPORH)^2$
HFU6	Green	0.78	$CKH = 0.6^2 \times CPORH^3 / 0.0314^2 / (1 - CPORH)^2$
HFU7	Brown	0.55	$CKH = 0.27^2 \times CPORH^3 / 0.0314^2 / (1 - CPORH)^2$
HFU8	Blue light		$CKH < 0.1mD$ and $CPORH < 4\%$

E. HFU Estimation in Un-Cored Well

The K.mod from Techlog is one of the best neural networks to generate the HFUs for the uncored sections. In this section, an association between well log response and core data for a

given set of experimental points is achieved. At first an adopted training model for well/log/EFs data and its associated FZI in a cored well is defined. Thus, we chose the model well for training. Then the method is generalized for the test wells to un-cored intervals to obtain HFU from its log and EF data. At the beginning, we subdivided the data into two classes, one for the training phase and another for the validation and application phase. The main inputs for the MLP are NPFI, GR, RHOB and EFs. The HFU values in the cored well are used as the output of the system. In this study, the network system comprises of one input layer, two hidden layers and one output layer (Figure 9). In the learning phase, we found that the mean squared error between the desired output and the calculated output is minimal for two hidden layers of 8 nodes. Figure 10 shows the results of the learning phase for one model well. HFUs-NN determined from MLP have a good match with HFU obtained from core porosity and core permeability. K-NN determined from MLP is correlated to core permeability with correlation coefficient (R^2) of 0.6. In the generalization phase, the network with eight nodes in the two-hidden layer gives minimal error. The generalization phase results by MLP for one test well is represented in Figure 11.

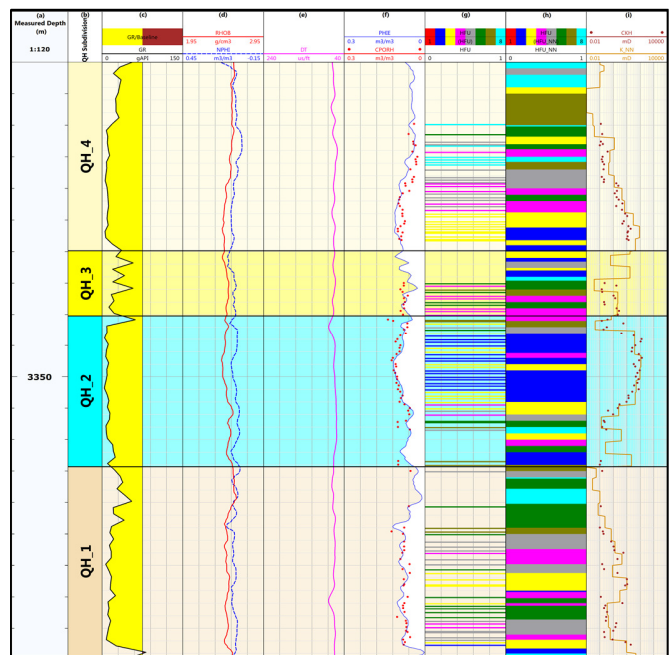


Fig. 10. HFUs results of the learning phase for one model well: (a) measured depth, (b) QH subdivision, (c) GR log, (d) RHOB and NPFI logs, (e) DT log, (f) core porosity and PHIE log, (g) distribution of HFUs in cored interval log, (h) distribution of HFU_NN using MLP, and (i) core permeability and predicted K-NN permeability using MLP.

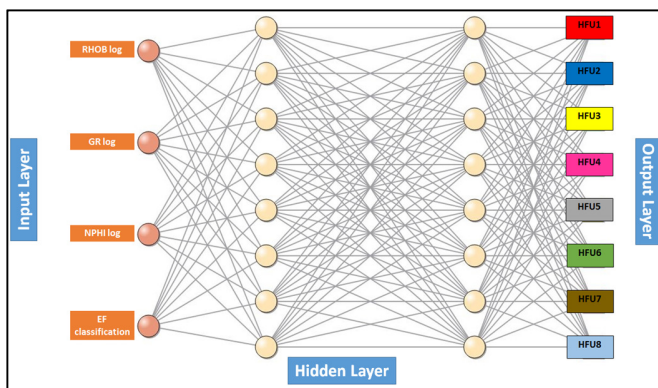


Fig. 9. MLP network architecture used for pilot wells

F. Saturation Height Modeling

Composite data containing SCAL data from one well are created and used for the saturation height modeling of the QH reservoir. Water saturation array is computed from this data set and plotted against PC curves in cross plot in order to examine each pressure curve separately. Some PCs are erroneous and not used. Lab capillary curves were converted to reservoir conditions (oil-brine) using (5):

$$PC_{res} = \frac{PC_{lab} * IFT_{res} * \cos \theta_{res}}{IFT_{lab} * \cos \theta_{lab}} \quad (5)$$

where PC_{res} is the oil brine capillary pressure reservoir in psia, PC_{lab} is the air brine capillary pressure in psia, IFT_{res} is the interfacial tension between oil and brine in dynes/cm (30), θ_{res} is the contact angle between oil and brine in degrees (30), IFT_{lab} is the interfacial tension between air and brine in dynes/cm (35) and $\cos \theta_{lab}$ is the contact angle between air and brine in degrees (0).

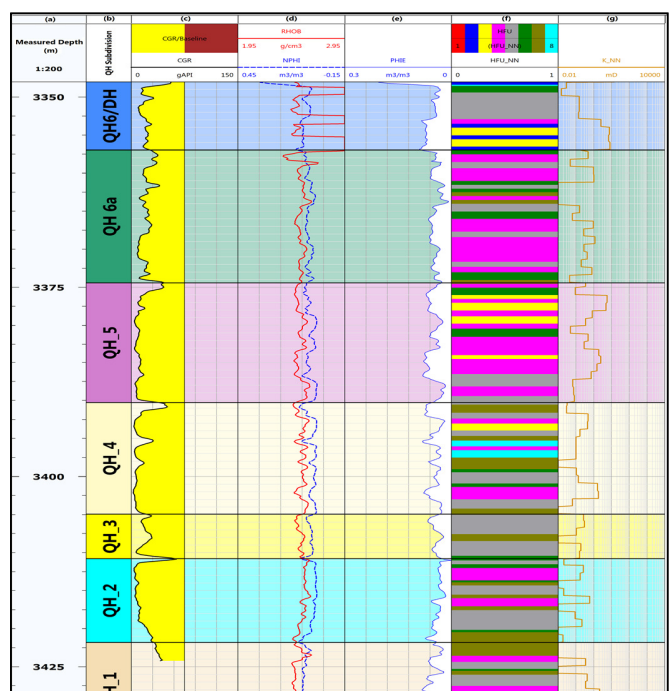


Fig. 11. HFUs results of the generalization phase for one test un-cored well: (a) measured depth, (b) QH subdivision, (c) CGR log, (d) RHOB and NPFI logs, (e) PHIE log, (f) distribution of HFU_NN using MLP, and (g) predicted K-NN permeability using MLP in un-cored interval.

The corrected capillary pressure curves at reservoir conditions were used to calculate one J-function per HFUs using the following equation:

$$J(S_w) = 0.2166 * \frac{P_c}{\sigma \cos \theta} * \sqrt{\frac{K}{\phi}} \quad (6)$$

where $J(S_w)$ is the Leverett capillary pressure function (unitless), P_c is the capillary pressure in psia, σ is the oil brine interfacial tension in dynes/cm (30), θ is the oil brine contact angle in degrees (30), ϕ is the porosity in fraction and K is the permeability in mD.

Techlog software is used for PC saturation height modeling. A single one best fit relationship between water saturation S_w and J-function (J) for each HFU is established in line with the below equations (Figure 12):

$$J(S_w)_{model} = \frac{1}{A} * (S_w - B)^{LAMBDA} \quad (7)$$

$$S_w(J)_{model} = A * J_{LEV}^{-LAMBDA} + B \quad (8)$$

where $J(S_w)$ is the Leverett capillary pressure function (unitless), $S_w(J)_{model}$ is the water saturation in fraction, A and $LAMBDA$ are coefficient determined by regression and B is the average irreducible water saturation for each HFU optimized using SCAL data.

Available PC data only covered HFU2 HFU3 and HFU4 for QH formation. Synthetic saturation height functions have to be generated for the rest of HFUs. To achieve this, the equation for HFU4 is used as starting point for the rather poorer HFUs and J-Leverett parameters A , B and $LAMBDA$ are iteratively adjusted until an acceptable match with log interpreted S_w is obtained. Functions are then checked and validated in Techlog to ensure that the shape of the original best fit curve to pc data is honored and not lost. HFU8 was considered as 100% water saturated or very bad quality reservoir. The obtained saturation height functions have a good match with S_w from logs. Figure 13 shows an example of the match obtained between saturation height model and log results for one well.

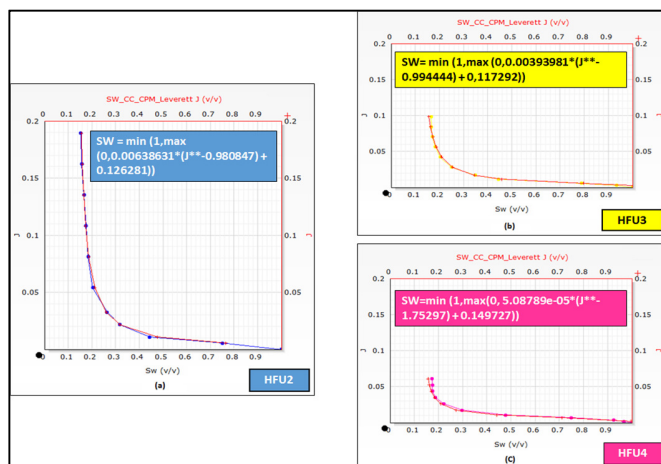


Fig. 12. Computed J-function and best fit (red) (QH, HMD oil field southern periphery)

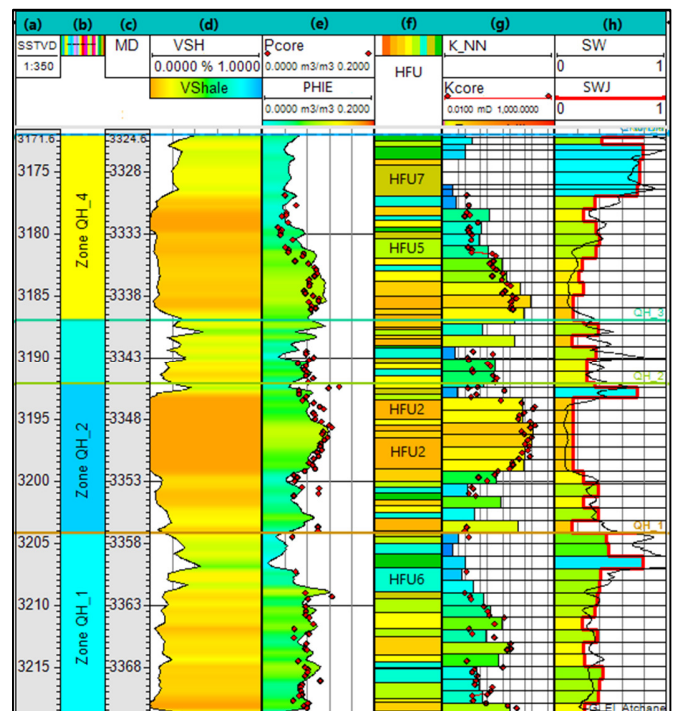


Fig. 13. Example of the obtained saturation height model with log results for one well: (a) True vertical sub sea measured depth, (b) QH subdivision, (c) measured depth, (d) VSH log, (e) core porosity and PHIE log, (e) HFU distribution, (f) core permeability and predicted K_NN permeability using MLP, and (g) J-function saturation and log saturation.

V. CONCLUSION

In this work, a workflow has been proposed to enhance rock type characterization. The best definition of rock type and saturation height functions requires some essential data such as RCA, SCAL and good quality logs. In this paper, an EF analysis is performed in the QH reservoir using an unsupervised neural network Kohonen algorithm. This analysis, carried out on fourteen wells, mainly based on logs, allowed us to define three EFs with a best reservoir quality (EF1, EF2 and EF3), one with moderate quality (EF4) and one with bad (EF5). A work based on the definition of the flow zone indicator (FZI) was applied in the QH reservoir. FZI is an adequate parameter for determining hydraulic flow units because it is based on pore throat network which controls fluid flow in the reservoir. Conventional core, SCAL and reservoir facies are integrated to define eight HFUs; The best HFUs are mainly located in the zones QH_2 and QH_4. Above these intervals, the bad rock types are dominant. This work proves that rock typing using FZI approach can be very efficient in building coherent and reliable permeability being necessary for reservoir characterization. In cored and un-cored intervals, a good agreement is obtained between core permeability and calculated K-NN permeability. Multi-layer perceptron is a robust and useful method to predict hydraulic flow unit in the un-cored intervals/wells.

PC curves are available for 3 HFUs: HFU2, HFU3 and HFU4. Thus, synthetic J-functions are generated for HFUs without PC curves. Finally, a good S_w match is obtained

between the model and the interpreted log results. For better estimation of saturation height functions, we suggest to take plugs for every HFU defined already. This analysis is going to allow us to avoid synthetic saturation height functions and therefore minimize the uncertainties on volumetric calculation. It's also recommended to measure in laboratory the oil brine interfacial tension and the contact angle.

REFERENCES

- [1] H. S. Naji, M. H. Hakimi, M. Khalil, F. A. Sharief, "Stratigraphy, deposition, and structural framework of the cretaceous (review) and 3D geological model of the lower cretaceous reservoirs, Masila oil field, Yemen", *Arabian Journal of Geosciences*, Vol. 3, No. 3, pp. 221-248, 2009
- [2] S. Benayad, Y. S. Yasbaa, C. R. Chaouchi, "Modeling of the Harma Quartzite Reservoir, Southern Periphery of the Hassi Messaoud Field, Saharan Platform", 79th European Association of Geoscientists & Engineers Conference and Exhibition, Paris, France, June 12-15, 2017
- [3] J. S. Gomes, M. T. Ribeiro, J. C. Strohmenger, S. Naghban, M. Z. Kalam, "Carbonate Reservoir Rock Typing-The Link Between Geology and SCAL", 13th Abu Dhabi International Petroleum Exhibition and Conference, Abu Dhabi, UAE, November 3-6, 2008
- [4] N. F. Alhashmi, K. Torres, M. Faisal, V. S. Cornejo, B. P. Bethapudi, S. Mansur, A. S. Al-Rawahi, "Rock Typing Classification and Hydraulic Flow Units Definition of One of the Most Prolific Carbonate Reservoir in the Onshore Abu Dhabi", SPE Annual Technical Conference and Exhibition, Dubai, UAE, September 26-28, 2016
- [5] A. Abedini, F. Torabi, P. Tontiwachwuthikul, "Reservoir rock type analysis using statistical pore size distribution", *Special Topics and Reviews in Porous Media: An International Journal*, Vol. 3, No. 2, pp. 97-103, 2012
- [6] Y. Li, R. A. Sprecher, "Facies identification from well logs: A comparison of discriminant analysis and Naïve Bayes classifier", *Journal of Petroleum Science and Engineering*, Vol. 53, No. 3-4, pp. 149-157, 2006
- [7] T. Kohonen, *Self-Organizing Maps*, Springer, 2001
- [8] S. A. Ouadfeul, N. Zaourar, A. Boudella, M. Hamoudi, "Modeling and classification of lithofacies using the continuous wavelet transform and neural network: A case study from Berkine Basin (Algeria)", *Bulletin du Service Geologique d'Algerie*, Vol. 22, No. 1, pp. 1-16, 2011
- [9] S. A. Ouadfeul, L. Aliouane, *Lithofacies Classification Using the Multilayer Perceptron and the Self-Organizing Neural Networks*, Springer, 2012
- [10] A. A. Moqbel, Y. Wang, "Carbonate reservoir characterization with lithofacies clustering and porosity prediction", *Journal of Geophysics and Engineering*, Vol. 8, No. 4, pp. 592-598, 2011
- [11] S. Haykin, *Neural Networks: A Comprehensive Foundation*, 2nd Edition, Prentice Hall, 1998
- [12] A. Astela, S. L. Tsakovski, P. Barbieri, V. Simeonov, "Comparison of self-organizing maps classification approach with cluster and principal components analysis for large environmental data sets", *Water Research*, Vol. 41, No. 19, pp. 4566-4578, 2007
- [13] R. Zabihi, M. Schaffie, M. Ranjbar, "The prediction of the permeability ratio using neural networks", *Energy Sources, Part A: Recovery, Utilization, and Environmental Effects*, Vol. 36, No. 6, pp. 650-660, 2014
- [14] S. Zerroug, N. Bounoua, R. Lounissi, R. Zeghouani, N. Djellas, K. Kartobi, A. Etchecopar, M. Mohamed Tchambaz, S. Abadir, P. Simon, J. Fuller, *Well Evaluation Conference Algeria*, Schlumberger, Lynx Consulting, 2007
- [15] A. A. Zoulikha, M. Djarir, R. Zenkhri, A. Sokhal, L. E. Hadi, A. Aguenini, G. Zandkarimi, P. Mosher, D. Xu, F. Likrama, E. E. Ahmed, M. Noaman, "Conducting Integrated Reservoir Studies in the Quartzite Hamra Reservoir-Tight Oil, Southern Periphery of Hassi Messaoud Field, Algeria", Annual Convention and Exhibition, Houston, Texas, United States, April 2-5, 2017
- [16] N. Kracha, *Relations Entre Sedimentologie, Fracturation Naturelle, et Diagenese d'un Reservoir a Faible Permeabilite: Application aux Reservoirs de l'Ordovicien du Bassin de l'Ahnnet, Sahara Central, Algerie*, PhD Thesis, Universite des Sciences et Technologies de Lille, 2011 (in French)
- [17] O. Serra, H. T. Abbott, "The contribution of logging data to sedimentology and stratigraphy", *Society of Petroleum Engineers Journal*, Vol. 22, No. 1, pp. 117-131, 1982
- [18] T. Kohonen, S. Kaski, H. Lappalainen, "Self-organized formation of various invariant feature filters in the adaptive-subspace SOM", *Neural Computation*, Vol. 9, No. 6, pp. 1321-1344, 1997
- [19] A. Niang, L. Gross, S. Thiria, F. Badran, C. Moulin, "Automatic neural classification of ocean color reflectance spectra at the top of the atmosphere with introduction of expert knowledge", *Remote Sensing of Environment*, Vol. 86, No. 2, pp. 257-271, 2003
- [20] J. O. Amaefule, M. Altunbay, D. Tiab, D. G. Kersey, D. K. Keelan, "Enhanced Reservoir Description: Using Core and Log Data to Identify Hydraulic (Flow) Units and Predict Permeability in Uncored Intervals/Wells", Annual Technical Conference and Exhibition, Houston, Texas, October 3-6, 1993
- [21] W. J. Ebanks, M. H. Scheihing, C. D. Atkinson, "Flow units for reservoir characterization, Part 6: Geological Methods", in: *Development Geology Reference Manual, AAPG Methods in Exploration Series*, No. 10, AAPG, 1992
- [22] F. A. A. Ajmi, S. A. Holditch, "Permeability Estimation Using Hydraulic Flow Units in a Central Arabia Reservoir", SPE Annual Technical Conference and Exhibition, Dallas, Texas, October 1-4, 2000
- [23] A. Sokhal, Z. Benaissa, S. A. Ouadfeul, A. Boudella, "Electrofacies Classification Using the Self-Organizing Map Approach with an Example from the Algerian Sahara", 19th EGU General Assembly, Vienna, Austria, April 23-28, 2017
- [24] A. Sokhal, S. A. Ouadfeul, S. Benmalek, "Rock Type and Permeability Prediction Using Flow-Zone Indicator with an Application to Berkine Basin (Algerian Sahara)", Society of Exploration Geophysicists, International Exposition and Annual Meeting, Dallas, USA, October 16-21, 2016
- [25] A. Sokhal, S. A. Ouadfeul, A. Bougandoura, "Fluid Flow Paths Discrimination in Tight Sand Gas Reservoirs Using the Hydraulic Flow Unit Approach with an Example from the Algerian Sahara", European Geosciences Union General Assembly, Vienna, Austria, April 12-17, 2015